

# Torsionally restricted tetradentate fluorophore: a swivelling ligand platform for ratiometric sensing of metal ions†

Xuan Jiang, Byung Gyu Park, Justin A. Riddle, Bong June Zhang, Maren Pink and Dongwhan Lee\*

Received (in Berkeley, CA, USA) 17th July 2008, Accepted 13th August 2008

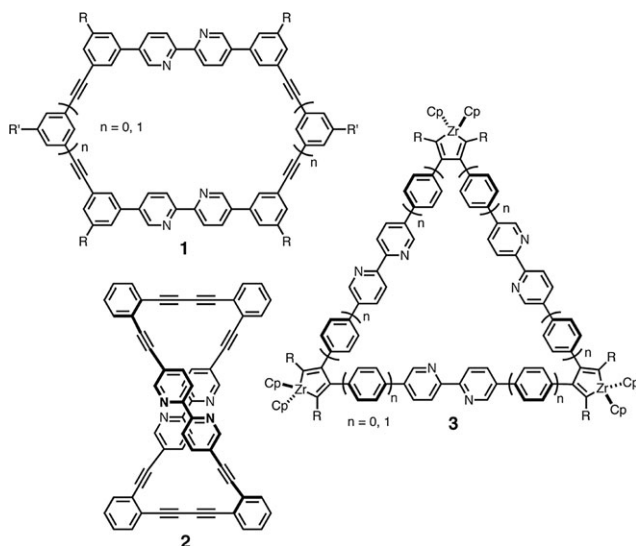
First published as an Advance Article on the web 14th October 2008

DOI: 10.1039/b812261j

A conformationally pre-organized ligand platform allows for restricted swivelling motions of two aryleneethynylene-appended 2,2'-bipyridyl units that function as a tight bischelator as well as a ratiometric fluorescence sensor for selected metal ions.

Cross-conjugated electronic structures continue to attract significant research interests in organic materials chemistry.<sup>1</sup> Molecular cruciforms represent one such architectural motif.<sup>2,3</sup> Spatial separation of the frontier molecular orbitals (FMOs) along each linear segment of such two-dimensional (2-D) constructs provides unique opportunities to control optoelectronic properties either through covalent modification of  $\pi$ -conjugated backbones<sup>4</sup> or by interaction with chemical input signal.<sup>5</sup>

Torsional control over the conjugation paths should directly impact the electronic properties associated with 2-D electronic conjugation.<sup>6</sup> This idea prompted us to explore a new  $\pi$ -conjugated platform that supports two converging 2,2'-bipyridyl (= bipy)<sup>7</sup> motifs. We report that this swivelling tetradentate ligand (i) displays fluorescence associated with cross-linked  $[n,\pi]/[\pi,\pi]$ -conjugation, (ii) tightly binds metal ions with  $K_a$  up to  $10^7 \text{ M}^{-1}$  to elicit red-shift in emission, and (iii) thus enables ratiometric fluorescence sensing.

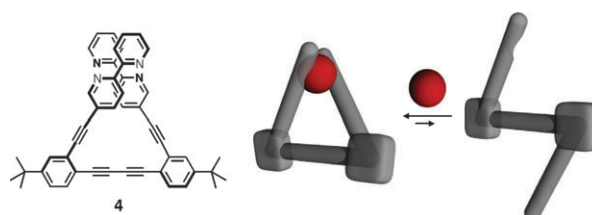


Department of Chemistry, Indiana University, 800 East Kirkwood Avenue, Bloomington, IN 47405, USA.

E-mail: dongwhan@indiana.edu; Fax: +1-812-855-8300;

Tel: +1-812-855-9364

† Electronic supplementary information (ESI) available: Experimental details for the synthesis, additional spectroscopic and crystallographic data. CCDC 695503 and 695504. For ESI and crystallographic data in CIF or other electronic format see DOI: 10.1039/b812261j

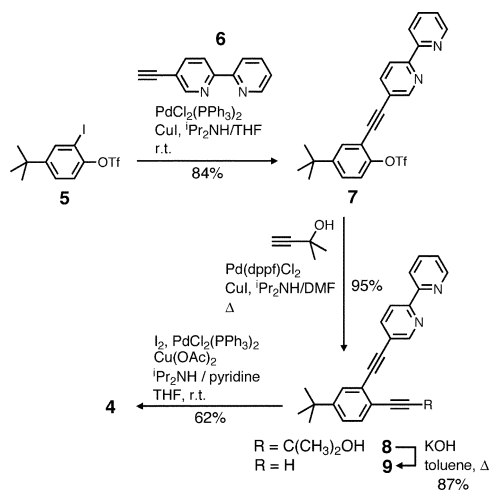


**Scheme 1** Chemical structure of **4** and schematic representation of metal binding through torsionally restricted structural folding.

Bipy-containing linearly conjugated structures have been extensively studied as fluorescence sensors for metal ions.<sup>8,9</sup> Efforts to incorporate bipy units into 2-D  $\pi$ -conjugated molecular scaffolds, however, focused predominantly on shape-persistent macrocycles<sup>10</sup> such as **1**,<sup>11</sup> **2**,<sup>12</sup> or **3**.<sup>13</sup>

We envisioned that a non-cyclic ligand **4** (Scheme 1) derived from **2** should have a limited number of freely rotating C–C bonds and thus provide finite trajectories for the two bipy fragments converging at the metal center. Such conformational restriction was anticipated to enhance the binding affinity by lowering the entropic cost of complexation. In addition, unique electronic properties associated with the  $[n,\pi]/[\pi,\pi]$ -conjugated molecular backbone could be exploited for optical signaling of such binding events.<sup>14</sup>

The molecular  $C_2$ -symmetry of **4** simplified the synthetic operation (Scheme 2), which commenced with Sonogashira–Hagihara coupling between **5** and 5-ethynyl-2,2'-bipyridine (**6**), proceeding exclusively on the iodo-substituted position of **5** to furnish the mono-coupled product **7**. A second round of



**Scheme 2** Synthetic route to **4**.

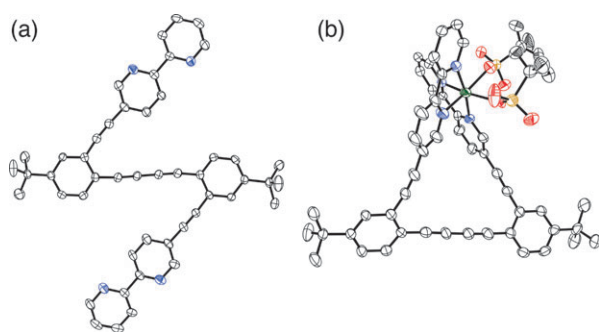


**Fig. 1** ORTEP diagrams of (a) **4** and (b) its Zn(II) complex [Zn(**4**)(OTf)<sub>2</sub>] with thermal ellipsoids at 50% probability, where N is blue, O is red, S is orange, and Zn is green. The *tert*-butyl groups of **4**, and one *tert*-butyl group and one OTf<sup>−</sup> ligand of [Zn(**4**)(OTf)<sub>2</sub>] are disordered over two positions, for which only one model is shown.

cross-coupling with acetone-protected acetylene produced **8**, which was subsequently converted to **9** under basic conditions. Oxidative homocoupling of **9** completed the synthesis of **4** (Fig. 1(a)).<sup>15</sup>

In MeCN at 298 K, **4** displayed a strong ( $\epsilon = 78\,000\text{ M}^{-1}\text{ cm}^{-1}$ ) absorption at  $\lambda_{\text{max}} = 310\text{ nm}$  and broad shoulders extending to *ca.* 400 nm (Fig. 2). In comparison, the UV-Vis spectrum of the “half-ligand” model **9** has no features above 360 nm, indicating that the optical transitions of **4** at the longer wavelength end originate from the  $\pi$ -conjugation along the diethynylene-linked biphenylene backbone. Consistent with this interpretation, the FMOs of **4** determined by density functional theory (DFT) calculations revealed significant electron delocalization along the extended ligand backbone (Fig. 3). On the other hand, the similarity between the strong absorption of **4** at  $\lambda_{\text{max}} = 310\text{ nm}$  and that of **6** at  $\lambda_{\text{max}} = 297\text{ nm}$  points toward  $\pi$ - $\pi^*$  electronic transitions localized at the ethynylbipyridyl “arm” fragment (Fig. 3). Accordingly, electronic perturbation induced by metal coordination should have profound effects on this region of the UV-Vis spectrum.

Addition of Zn<sup>2+</sup> (delivered as triflate salt) to **4** in MeCN indeed elicited a gradual decrease in intensity of the absorption peak at  $\lambda_{\text{max}} = 310\text{ nm}$  with concomitant development of a longer wavelength transition at  $\lambda_{\text{max}} = 327\text{ nm}$  (Fig. S1, ESI<sup>†</sup>). The well-resolved isosbestic point at  $\lambda = 319\text{ nm}$  suggested the formation of a discrete metal complex of **4**, the 1 : 1 binding stoichiometry of which was subsequently confirmed by the Job’s plot analysis (Fig. S2, ESI<sup>†</sup>). In contrast, the half-ligand model **9** displayed complicated binding patterns as reflected on

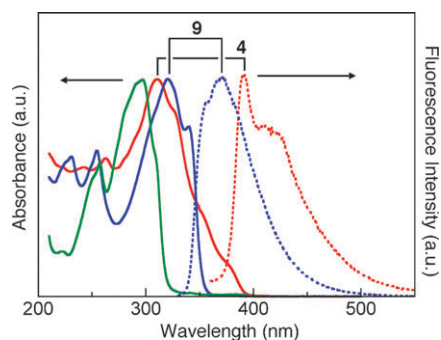


**Fig. 2** Normalized UV-Vis (solid lines) and fluorescence (dotted lines) spectra of **4** (red), **6** (green) and **9** (blue) in MeCN,  $T = 298\text{ K}$ .

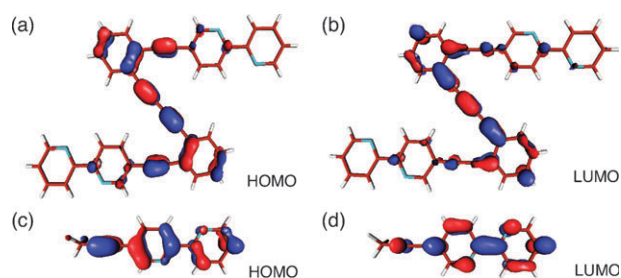


**Fig. 3** FMO isosurface plots (isodensity value = 0.05 au) of DFT models of **4** (a and b) and **6** (c and d).

the Job plot (Fig. S3, ESI<sup>†</sup>), which pointed toward the formation of multiple competing species in solution.

A high binding constant ( $K_a$ ) of  $1.7 (\pm 0.5) \times 10^7\text{ M}^{-1}$  (in MeCN) was obtained by fitting  $\Delta A_{310}$  vs. [Zn<sup>2+</sup>] data against a typical 1 : 1 binding isotherm. Under similar conditions, systematically weaker binding was observed for Cd<sup>2+</sup> and Hg<sup>2+</sup>, with  $K_a = 1.5 (\pm 0.5) \times 10^6\text{ M}^{-1}$  and  $9.4 (\pm 0.9) \times 10^4\text{ M}^{-1}$ , respectively (Fig. S4 and S5, ESI<sup>†</sup>). The decrease in the binding affinity along the series Zn<sup>2+</sup> > Cd<sup>2+</sup> > Hg<sup>2+</sup> might be rationalized by the inability of the torsionally restricted ligand **4** to fully relax to accommodate metals of larger ionic radii. Alternatively, increasing softness of the d<sup>10</sup> metals down the row might weaken the M–N<sub>imine</sub> bonds.

Structural preorganization of **4** apparently plays a critical role in discrete 1 : 1 complexation with high binding constants. This was subsequently confirmed by X-ray crystallography on its Zn<sup>2+</sup> complex.† As shown in Fig. 1(b), **4** supports a six-coordinate metal center with bis(bipy)-derived four nitrogen atoms adopting a *cis*-divacant octahedral geometry and two triflate-derived oxygen atoms completing the remaining coordination sites. Metal binding proceeds *via* rigid body swiveling motions of the *ortho*-phenyleneethynylenebipyridyl arms around the diethynylene hinge of **4** with no significant structural distortion of the molecular backbone.

In addition to providing a torsionally restricted structural platform for high-affinity binding, the bent [n, $\pi$ ]-system of **4** fundamentally switched the intrinsic de-excitation mechanism of the bipy unit. The free ligand **4** in MeCN at 293 K showed fluorescence peaks at  $\lambda_{\text{max}} = 390$  and 415 nm with a large Stokes shift (Fig. 2). Addition of Zn<sup>2+</sup>, however, elicited a significant decrease in the free-ligand emission with a concomitant development of the intense ligand–metal complex emission at 495 nm with an isoemissive point at 433 nm

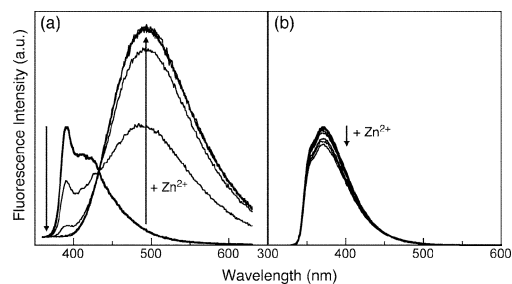


**Fig. 4** Fluorescence response of (a) **4** (0.5  $\mu\text{M}$ ) and (b) **9** (1.0  $\mu\text{M}$ ) upon addition of Zn<sup>2+</sup> (0–2.5  $\mu\text{M}$ ) in MeCN with  $\lambda_{\text{exc}} = 320\text{ nm}$ ;  $T = 293\text{ K}$ . Each trace corresponds to a 0.5  $\mu\text{M}$  increment of [Zn<sup>2+</sup>].

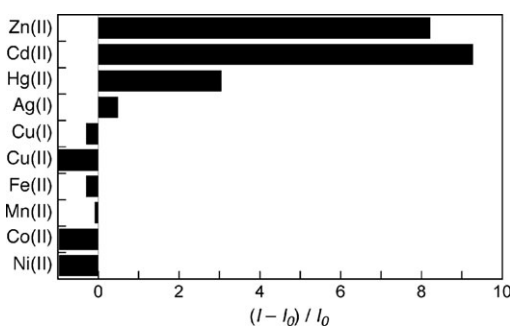


**Fig. 5** Fluorescence response of **4** (0.5  $\mu\text{M}$ ) toward various transition-metal ions (2.5  $\mu\text{M}$ ) in MeCN. The response was quantified by the ratio  $(I - I_0)/I_0$ , in which  $I_0$  and  $I$  denote the emission intensity at  $\lambda = 500$  nm prior to and after addition of the metal ion, respectively;  $\lambda_{\text{exc}} = 320$  nm;  $T = 293$  K.

(Fig. 4(a)). The ratio of  $I_{500}/I_{390}$  with excitation at 320 nm varied from 0.1 in the absence of  $\text{Zn}^{2+}$  to 25 upon treatment of 5 equiv.  $\text{Zn}^{2+}$  (2.5  $\mu\text{M}$ ), a 250-fold emission ratio increase. Under similar conditions, the half-ligand model **9** showed only slight decrease in the intensity of the  $\lambda = 370$  nm peak with no development of longer wavelength features (Fig. 4(b)). On the other hand, the bipy ligand fragment model **6** showed a simple fluorescence turn-on behavior toward  $\text{Zn}^{2+}$  (Fig. S6, ESI<sup>†</sup>). The significant enhancement and red-shift in the emission of **4** now enables ratiometric detection, which is advantageous over conventional measurement at a single wavelength.<sup>8,16–20</sup>

The high affinity of **4** toward group 12 metal ions prompted the investigation of its response profile across a wider range of transition-metal ions. As summarized in Fig. 5, a MeCN solution of **4** (0.5  $\mu\text{M}$ ) displayed strong turn-on fluorescence response toward  $\mu\text{M}$ -level concentrations of  $\text{Zn}^{2+}$ ,  $\text{Cd}^{2+}$  and  $\text{Hg}^{2+}$  as monitored by changes in the emission intensity. On the other hand, other closed-shell ions such as  $\text{Ag}^+$  or  $\text{Cu}^+$ , or paramagnetic  $\text{Cu}^{2+}$ ,  $\text{Fe}^{2+}$ ,  $\text{Mn}^{2+}$ ,  $\text{Co}^{2+}$  or  $\text{Ni}^{2+}$  elicited either complete quenching or negligible changes.<sup>21</sup>

In summary, a new dynamic fluorophore was prepared, in which swivelling motions around a rigid  $\pi$ -conjugated axle was exploited to enforce two metal binding units to converge at the metal center as a tight bischelator. A high affinity binding with  $K_a$  up to  $\sim 10^7$   $\text{M}^{-1}$  and ratiometric fluorescence response toward selected metal ions promise potential application of this and related ligand platforms for biological and environmental sensing.<sup>20,22–24</sup> Efforts are currently underway in order to improve the selectivity, sensitivity, and solubility of this first-generation prototype in aqueous environments.

This work was supported by the National Science Foundation (CAREER CHE 0547251) and the US Army Research Office (W911NF-07-1-0533). This paper is dedicated to Professor Myunghyun Paik Suh on the occasion of her 60th birthday.

## Notes and references

<sup>†</sup> Crystal data for  $[\text{Zn}(\mathbf{4})(\text{OTf})_2]$ :  $\text{C}_{50}\text{H}_{38}\text{F}_6\text{N}_4\text{O}_6\text{S}_2\text{Zn}$ ,  $M = 1034.33$ , monoclinic, space group  $C2/c$ ,  $a = 59.348(3)$ ,  $b = 9.9017(6)$ ,  $c = 19.2658(12)$  Å,  $\beta = 102.291(2)^\circ$ ,  $V = 11062.0(11)$  Å<sup>3</sup>,  $T = 150(2)$  K,  $Z = 8$ , 35934 reflections measured, 9700 unique

( $R_{\text{int}} = 0.0745$ ). Final  $\text{Goof} = 0.946$ ,  $R1 = 0.0690$ ,  $wR2 = 0.1800$  (with  $I > 2\sigma(I)$ ).

- (a) *Organic Electronics*, ed. H. Klauk, Wiley-VCH, Weinheim, Germany, 2006; (b) *Functional Organic Materials*, ed. T. J. J. Müller and U. H. F. Bunz, Wiley-VCH, Weinheim, 2007; (c) M. Gholami and R. R. Tykwinski, *Chem. Rev.*, 2006, **106**, 4997.
- F. Galbrecht, T. W. Bünnagel, A. Bilge, U. Scherf and T. Farrell, in *Functional Organic Materials*, ed. T. J. J. Müller and U. H. F. Bunz, Wiley-VCH, Weinheim, 2007, pp. 83–118.
- For conceptually related “H-shaped” 2-D conjugation, see: N. Zhou, L. Wang, D. W. Thompson and Y. Zhao, *Org. Lett.*, 2008, **10**, 3001.
- (a) J. A. Marsden, J. J. Miller, L. D. Shirtcliff and M. M. Haley, *J. Am. Chem. Soc.*, 2005, **127**, 2464; (b) C.-H. Zhao, A. Wakamiya, Y. Inukai and S. Yamaguchi, *J. Am. Chem. Soc.*, 2006, **128**, 15934.
- (a) J. N. Wilson and U. H. F. Bunz, *J. Am. Chem. Soc.*, 2005, **127**, 4124; (b) A. J. Zuccherro, J. N. Wilson and U. H. F. Bunz, *J. Am. Chem. Soc.*, 2006, **128**, 11872; (c) S. M. Brombosz, A. J. Zuccherro, R. L. Phillips, D. Vazquez, A. Wilson and U. H. F. Bunz, *Org. Lett.*, 2007, **9**, 4519; (d) E. L. Spitzer, L. D. Shirtcliff and M. M. Haley, *J. Org. Chem.*, 2007, **72**, 86; (e) P. L. McGrier, K. M. Solntsev, J. Schönhaber, S. M. Brombosz, L. M. Tolbert and U. H. F. Bunz, *Chem. Commun.*, 2007, 2127.
- E. Opsitnick and D. Lee, *Chem.–Eur. J.*, 2007, **13**, 7040.
- C. Kaes, A. Katz and M. W. Hosseini, *Chem. Rev.*, 2000, **100**, 3553.
- (a) A. Ajayaghosh, P. Carol and S. Sreejith, *J. Am. Chem. Soc.*, 2005, **127**, 14962; (b) A. E. Dennis and R. C. Smith, *Chem. Commun.*, 2007, 4641.
- (a) B. Wang and M. R. Wasielewski, *J. Am. Chem. Soc.*, 1997, **119**, 12; (b) A. Kokil, P. Yao and C. Weder, *Macromolecules*, 2005, **38**, 3800; (c) L. Tian, W. Zhang, B. Yang, P. Lu, M. Zhang, D. Lu, Y. Ma and J. Shen, *J. Phys. Chem. B*, 2005, **109**, 6944.
- (a) D. Zhao and J. S. Moore, *Chem. Commun.*, 2003, 807; (b) S. Höger, *Chem.–Eur. J.*, 2004, **10**, 1320.
- (a) O. Henze, D. Lentz and A. D. Schlüter, *Chem.–Eur. J.*, 2000, **6**, 2362; (b) O. Henze, D. Lentz, A. Schäfer, P. Franke and A. D. Schlüter, *Chem.–Eur. J.*, 2002, **8**, 357; (c) D. M. Opris, P. Franke and A. D. Schlüter, *Eur. J. Org. Chem.*, 2005, 822; (d) D. M. Opris, A. Ossensbach, D. Lentz and A. D. Schlüter, *Org. Lett.*, 2008, **10**, 2091.
- P. N. W. Baxter, *J. Org. Chem.*, 2001, **66**, 4170.
- (a) J. Nitschke and T. D. Tilley, *J. Org. Chem.*, 1998, **63**, 3673; (b) J. R. Nitschke, S. Zürcher and T. D. Tilley, *J. Am. Chem. Soc.*, 2000, **122**, 10345; (c) J. R. Nitschke and T. D. Tilley, *Angew. Chem., Int. Ed.*, 2001, **40**, 2142.
- Coordination-induced spectral changes have previously been reported for **2** but no information is available for its binding stoichiometry, affinity, or the structure of putative metal complexes<sup>12</sup>.
- A pyrene-appended all-carbon analogue of **4** was recently reported. See: S. Sankararaman, G. Venkataramana and B. Varghese, *J. Org. Chem.*, 2008, **73**, 2404.
- M. M. Henary, Y. Wu and C. J. Fahrni, *Chem.–Eur. J.*, 2004, **10**, 3015.
- M. Taki, J. L. Wolford and T. V. O'Halloran, *J. Am. Chem. Soc.*, 2004, **126**, 712.
- C. J. Chang, J. Jaworski, E. M. Nolan, M. Sheng and S. J. Lippard, *Proc. Natl. Acad. Sci. USA*, 2004, **101**, 1129.
- E. M. Nolan and S. J. Lippard, *J. Am. Chem. Soc.*, 2007, **129**, 5910.
- D. W. Domaille, E. L. Que and C. J. Chang, *Nat. Chem. Biol.*, 2008, **4**, 168.
- Fluorescence quenching by paramagnetic or heavy metal ions has typically been ascribed to the effect of strong spin–orbit coupling. Closed-shell metal ions suffer less from such deleterious pathways and (with appropriate metal–fluorophore combinations) can give rise to enhanced emission through the inversion of the  $\pi\pi^*$ – $\pi\pi^*$  ligand excited states<sup>22</sup>.
- A. P. de Silva, H. Q. N. Gunaratne, T. Gunnlaugsson, A. J. M. Huxley, C. P. McCoy, J. T. Rademacher and T. E. Rice, *Chem. Rev.*, 1997, **97**, 1515.
- S. W. Thomas III, G. D. Joly and T. M. Swager, *Chem. Rev.*, 2007, **107**, 1339.
- J. S. Kim and D. T. Quang, *Chem. Rev.*, 2007, **107**, 3780.